



## Formation of incipient anodes in localized mortar repairs with the addition of rice husk silica

I. R. Remenche<sup>1\*</sup>, P. A. Daschevi<sup>2</sup> , N. F. Holowka<sup>3</sup>, L. C. Martioli<sup>1</sup>, M. H. F. Medeiros<sup>1</sup> 

\*Contact author: [igorrossi@ufpr.br](mailto:igorrossi@ufpr.br)

DOI: <https://doi.org/10.21041/ra.v14i3.763>

Received: 01/06/2024 | Received in revised form: 02/08/2024 | Accepted: 20/08/2024 | Published: 01/09/2024

### ABSTRACT

The objective of this work was to investigate how incipient anodes can be detected and monitored in localized repair areas using mortars with added rice husk silica. Three repair conditions were tested on prismatic specimens: without repair, with repair without rice husk silica addition, and with rice husk silica addition in the mortar. Corrosion potential and electrical resistivity tests were conducted. The corrosion potential test showed no variation along the bar, while the electrical resistivity test showed varied values depending on the repaired and non-repaired zones. It was concluded that adding rice husk silica to the mortar made the corrosion potential more electronegative due to the greater difference in electrical resistivity compared to the substrate, contributing to the formation of incipient anodes.

**Keywords:** incipient anode; electrochemical incompatibility; repair; corrosion potential; surface electrical resistivity.

**Cite as:** Remenche, I. R., Daschevi, P. A., Holowka, N. F., Martioli L. C., Medeiros, M. H. F. (2024), " *Formation of incipient anodes in localized mortar repairs with the addition of rice husk silica* " Revista ALCONPAT, 14 (3), pp. 255 – 274, DOI: <https://doi.org/10.21041/ra.v14i3.763>

<sup>1</sup> Program of Graduate Studies in Civil Engineering, Federal University of Paraná (UFPR), Curitiba, Brazil.

<sup>2</sup> Court of Accounts of Paraná, Curitiba, Brazil.

<sup>3</sup> Program of Graduate Studies in Civil Engineering, Federal Technological University of Paraná (UTFPR), Curitiba, Brazil.

### Contribution of each author

In this work, the author I. R. Remenche contributed to data collection (50%), literature review (50%), and writing (60%). The author P. A. Daschevi contributed with the original idea and review of the work. The author N. F. Holowka participated in data collection (50%). The author L. C. Martioli contributed to the preparation of the images and literature review (20%). The author M. H. F. Medeiros collaborated in the writing (40%), literature review (30%), and as a supervisor and overall reviewer of the work.

### Creative Commons License

Copyright 2024 by the authors. This work is an Open-Access article published under the terms and conditions of an International Creative Commons Attribution 4.0 International License ([CC BY 4.0](https://creativecommons.org/licenses/by/4.0/)).

### Discussions and subsequent corrections to the publication

Any dispute, including the replies of the authors, will be published in the second issue of 2025 provided that the information is received before the closing of the first issue of 2025.

## Formação de ânodos incipientes em reparos localizados de argamassa com adição de sílica de casca de arroz

### RESUMO

O objetivo deste trabalho foi investigar como o ânodo incipiente pode ser detectado e monitorado em áreas de reparo localizado com argamassas contendo adição de sílica de casca de arroz. Foram testadas três condições de reparo em corpos de prova prismáticos: sem reparo, com reparo sem adição de sílica de casca de arroz e com adição de sílica de casca de arroz na argamassa. Realizaram-se ensaios de potencial de corrosão e resistividade elétrica. O ensaio de potencial de corrosão não apresentou variação ao longo da barra, enquanto o ensaio de resistividade elétrica apresentou valores variados em função da zona reparada e não reparada. Concluiu-se que a adição de sílica de casca de arroz na argamassa tornou o potencial de corrosão mais eletronegativo devido à maior diferença de resistividade elétrica em relação ao substrato, contribuindo para a formação do ânodo incipiente.

**Palavras-chave:** ânodo incipiente; incompatibilidade eletroquímica; reparo; potencial de corrosão e resistividade elétrica superficial.

## Formación de ánodos incipientes en reparaciones localizadas de morteros con adición de sílice de cáscara de arroz

### RESUMEN

El objetivo de este trabajo fue investigar cómo se puede detectar y monitorear el ánodo incipiente en áreas de reparación localizadas con morteros que contienen adición de sílice de cáscara de arroz. Se probaron tres condiciones de reparación en probetas prismáticas: sin reparación, con reparación sin adición de sílice de cáscara de arroz y con adición de sílice de cáscara de arroz en el mortero. Se realizaron pruebas de potencial de corrosión y resistividad eléctrica. La prueba de potencial de corrosión no mostró variación a lo largo de la barra, mientras que la prueba de resistividad eléctrica mostró valores variables dependiendo del área reparada y no reparada. Se concluyó que la adición de sílice de cáscara de arroz al mortero hizo que el potencial de corrosión fuera más electronegativo debido a la mayor diferencia de resistividad eléctrica con relación al sustrato, contribuyendo a la formación del ánodo incipiente.

**Palabras clave:** ánodo incipiente; incompatibilidad electroquímica; reparar; potencial de corrosión y resistividad eléctrica de la superficie.

### Legal Information

Revista ALCONPAT is a quarterly publication by the Asociación Latinoamericana de Control de Calidad, Patología y Recuperación de la Construcción, Internacional, A.C., Km. 6 antigua carretera a Progreso, Mérida, Yucatán, 97310, Tel.5219997385893, [alconpat.int@gmail.com](mailto:alconpat.int@gmail.com), Website: [www.alconpat.org](http://www.alconpat.org)

Reservation of rights for exclusive use No.04-2013-011717330300-203, and ISSN 2007-6835, both granted by the Instituto Nacional de Derecho de Autor. Responsible editor: Pedro Castro Borges, Ph.D. Responsible for the last update of this issue, ALCONPAT Informatics Unit, Elizabeth Sabido Maldonado.

The views of the authors do not necessarily reflect the position of the editor.

The total or partial reproduction of the contents and images of the publication is carried out in accordance with the COPE code and the CC BY 4.0 license of the Revista ALCONPAT.

## 1. INTRODUCTION

According to the NACE International report (2016), it is estimated that global corrosion expenses amount to 2.5 trillion dollars, corresponding to 3.4% of the global GDP. The same source proposes that if corrosion control practices were adopted, savings could range from 15% to 35%, equivalent to 375 to 875 billion dollars annually. In Brazil, the losses due to corrosion in 2015 represented 4% of the GDP, equivalent to R\$ 236 billion (Grandes Construções, 2017).

Regarding steel in reinforced concrete structural elements, Mehta and Monteiro (2008) originally believed that reinforcement protected from direct air contact by a layer of Portland cement concrete with low capillary porosity would not suffer corrosion or present pathological manifestations. However, in practice and over the years, it has been observed that this assumption does not hold, as durability problems contradict this evidence. Thus, it became evident that in reinforced concrete structures, steel corrosion can worsen in the early stages of service life, even when the concrete is dense and adequately mixed.

In this context, the understanding has developed that reinforced concrete structures need a long and consistent service life to avoid a drastic reduction in properties related to durability, avoiding increased material consumption in the construction industry and additional expenses with early repairs. On this subject, according to Krishnan *et al.* (2021), the NACE Impact Report (2016) indicates that about 50% of reinforced concrete structures need to be repaired within 10 years after construction. Generally, the adopted solution is localized repairs.

Thus, regarding the repair of reinforced concrete structures, there is a technique for localized repair of corroded areas, with standardized procedures and traditional and innovative materials proposed over the decades. However, in practical conditions, it is common to find repair failures within a few years, requiring rework and the application of new materials, leading to increased material consumption and environmental impact.

In summary, conventional repairs in many structures are failing within about 5 years, necessitating repeated repairs and significantly increasing the total cost of corrosion and the life cycle cost of reinforced concrete structures. The reasons for premature failures include a lack of technical rigor in execution, incorrect material specification, and cost-saving measures in repair systems (incomplete repairs to reduce cost), failing to fully stop the installed corrosion process.

In this context, it is known that corrosion in repaired structures tends to restart mainly at the interface between the old concrete and the repaired area, leading to the formation of incipient anodes. Thus, corrosion can continue to progress within the concrete, even after a deteriorated section of concrete has been removed and replaced with a new repair material.

Several studies have aimed to understand the formation of incipient anodes in localized repairs, the effects caused by this pathological manifestation, and methods to mitigate them (Castro *et al.*, 2003; Christodoulou *et al.*, 2013; Luković *et al.*, 2017; Ali *et al.*, 2018; Kamde *et al.*, 2021). In this context, Castro *et al.* (2003) analyzed prismatic samples with localized repairs in concrete contaminated with 0.7% chloride by mass. The authors evaluated four systems for the repair region: (1) only alkaline repassivation in the repaired area, (2) application of a single-component primer with zinc-rich epoxy resin, and (3-4) two different two-component primers.

Christodoulou *et al.* (2013) studied localized repairs in field structures, specifically a multi-story parking garage exposed to chloride attack and a reinforced concrete bridge with multiple spans. The authors performed repairs in deteriorated concrete areas using three different materials to observe the formation of incipient anodes: a flowable micro-concrete based on Portland cement, polymer-modified and shrinkage-compensated; a repair mortar based on Portland cement, polymer-modified, shrinkage-compensated with added silica fume; and a non-shrink repair mortar based on magnesia-phosphate cement.

Subsequently, Luković *et al.* (2017) expanded this research by evaluating the applicability of strain-hardening cementitious composites (SHCC) in repairs subjected to ongoing corrosion, as

well as studying the use of non-reinforced repair mortars and commercial repair materials. Meanwhile, Ali *et al.* (2018) investigated various repair strategies available on the market using prismatic samples exposed to different conditions with and without chlorides.

Therefore, this study aims to evaluate the effects of the presence of localized repairs with the incorporation of rice husk silica on the formation of incipient anodes. For this purpose, two exposure conditions were considered in the preparation of the specimens: one group contaminated with chlorides and another uncontaminated. Furthermore, the study analyzed three different repair scenarios: the concrete piece without repair, as well as specimens repaired with pure Portland cement mortar and specimens repaired with mortar containing rice husk silica (RHS) in the binder composition. Two non-destructive tests were also conducted to evaluate the structural element's integrity: corrosion potential ( $E_{\text{corr}}$ ) and surface electrical resistivity. The analysis aimed to contribute to verifying the formation of incipient anodes in concrete with added rice husk silica and to investigate whether the pozzolanic activity intensifies the corrosion process due to the formation of incipient anodes.

To achieve this, the theoretical foundation supporting the analysis, the methods used in the investigation to determine the presence of incipient anodes, the analysis results, and the discussion of the data were presented, followed by the conclusions.

## 2. FORMATION OF INCIPIENT ANODES

When localized repair services are performed, it is common to remove concrete that shows cracks or fissures and even contamination with chlorides. Therefore, it is necessary to clean the steel bar and replace the old concrete with a new composite called repair material. However, even after the repair, corrosion may continue. This is due to the difference in electrochemical behavior between the old and new concrete, improperly cleaned reinforcement, high concrete permeability, etc.

Thus, the "Incipient Anode Effect" is an important phenomenon to consider in the context of localized mortar repairs in a reinforced concrete piece, especially when dealing with steel reinforcement corrosion.

The term "incipient anode" refers to a localized area at the interface between the concrete and the structural repair, leading to the formation of the active corrosion process of the reinforcement (Luković *et al.*, 2017; Ali *et al.*, 2018). This area becomes a focal point for corrosive attack and can be characterized by certain conditions conducive to forming a galvanic cell, such as the difference between the electrochemical characteristics of the steel reinforcement in the original concrete and the repaired area, necessitating repeated repairs due to the occurrence of early failures (Kamde *et al.*, 2021).

The incipient anode is critical in the context of reinforced concrete repairs because if not properly addressed, it can lead to future durability problems. During the repair, it is essential to identify and treat all areas affected by corrosion, which generally involves complete removal of the corroded area, proper surface preparation, and the application of protective measures such as coatings, galvanic anodes, or even corrosion inhibitors.

For this purpose, localized repairs in structural elements are a commonly found technique in buildings in Brazil. The technique aims to interrupt the electrochemical cell generated over the service life of the piece and restore the steel's passivating layer through the application of new concrete, grout, or repair mortar. Despite proper repair execution, steel corrosion at the interface between the concrete and repair mortar can still be observed (Medeiros, Daschevi, Araújo, 2022). Figure 1 shows the incipient anode effect in corrosion potential tests on structural elements.

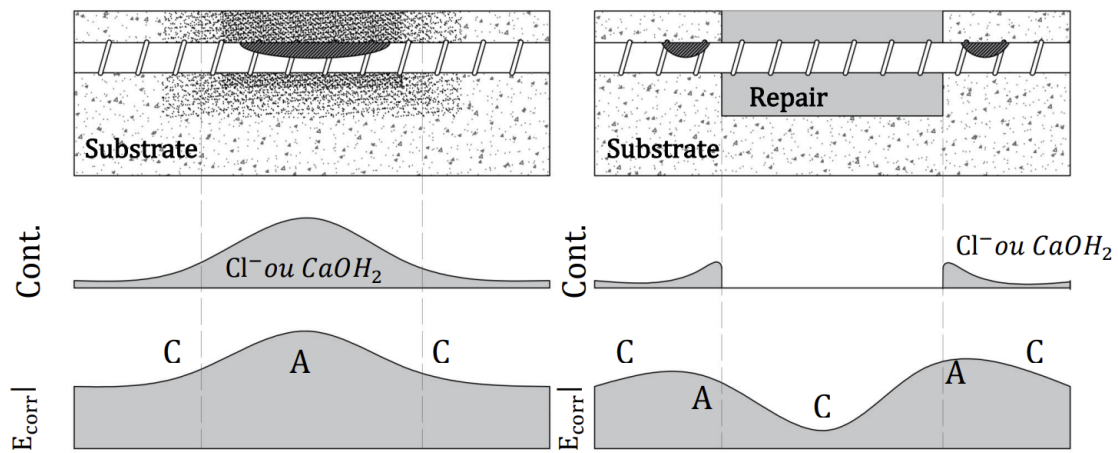


Figure 1. Classic configurations of corrosion potential variation when incipient anodes form in repaired elements.

Source: Medeiros, Daschevi, and Araújo (2022).

It can be observed that, in the first situation, the reinforcement is corroding in the middle, and, as a result, the corrosion potential (in magnitude) in that region is higher than in the other areas. However, in the second case, the interface where the repair was performed shows peaks in corrosion potential, while in the middle of the repair, the reinforcement would be in a passive condition.

Thus, using appropriate repair materials can permanently decrease the corrosion potential of steel within the repair area. The reasons for this would be the typically low permeability and the high pH of these materials. A high pH in the newly repaired area results in a negative change because the equilibrium potentials of the steel in the concrete would be more negative than in the newly repaired region (Christodoulou *et al.*, 2013).

Therefore, the early detection of incipient anodes is crucial for the maintenance and preservation of reinforced concrete structures, as corrective measures can be taken to stop the corrosive process before it causes significant damage. This may involve the application of protective coatings, cathodic protection, repair of corroded areas with mortar, and environmental control.

### 3. EXPERIMENTAL METHODOLOGY

#### 3.1 Characterization of Materials

The Portland cement used in the experimental program was CP V – ARI type for concrete and repair mortars. This cement meets the requirements established in NBR 16697 (ABNT, 2018). Table 1 shows the chemical, physical, and mechanical characterization data of this cement.

Table 1. Chemical, physical, and mechanical characterization of CP V – ARI cement.

Chemical composition (%)										
CaO	SiO <sub>2</sub>	Al <sub>2</sub> O <sub>3</sub>	Fe <sub>2</sub> O <sub>3</sub>	SO <sub>3</sub>	MgO	Free CaO	Alkali Equivalent	Insoluble Residue	Loss on Ignition	
62.20	19.82	4.49	3.05	2.74	2.02	1.02	0.66	0.63	3.41	
Expan. (%)	Setting Time (min)		Blaine Fineness (cm <sup>2</sup> /g)	#200 (%)	#325 (%)	Compressive Strength (MPa)				Specific Mass (g/cm <sup>3</sup> )
	Initial	Final				1 day	3 days	7 days	28 days	
0.18	217	267	4366	0.05	0.35	23.4	38.1	44.5	52.5	3.09

Source: Manufacturer.

As a pozzolanic addition, rice husk silica (RHS) was used, chemically characterized in Table 2. This mineral addition was obtained from controlled burning in a fluidized bed system to produce a material with optimized pozzolanicity. To measure the pozzolanic capacity of this addition, the Modified Chapelle test was conducted, following NBR 15895 (ABNT, 2010), which establishes that for classification as a pozzolan, the minimum calcium hydroxide consumption should be 436 mg Ca(OH)<sub>2</sub>/g of addition.

In this case, rice husk silica fixed lime at 1336 mg Ca(OH)<sub>2</sub>/g sample, well above the minimum limit established in NBR 15895 (ABNT, 2010), classifying this material as highly reactive.

Table 2. Chemical properties of rice husk silica (RHS).

Chemical Composition (%)									Other Properties		
CaO	SiO <sub>2</sub>	Al <sub>2</sub> O <sub>3</sub>	Fe <sub>2</sub> O <sub>3</sub>	MgO	SO <sub>3</sub>	K <sub>2</sub> O	Other Oxides	Loss on Ignition	BET surface area	Specific Mass (g/cm <sup>3</sup> )	Modified Chapelle (mg Ca(OH) <sub>2</sub> /g addition)
0.43	88.47	2.72	0.05	-	1.55	1.46	0.49	4.84	14,692	2.12	1336
*CuO, ZnO, MnO, P <sub>2</sub> O <sub>5</sub> , Tm <sub>2</sub> O <sub>3</sub> and Rb <sub>2</sub> O											

Figure 2 shows the X-ray diffraction pattern, indicating the presence of a mineral portion in the amorphous state, with cristobalite crystalline phase peaks and an amorphous halo typical of pozzolanic material.

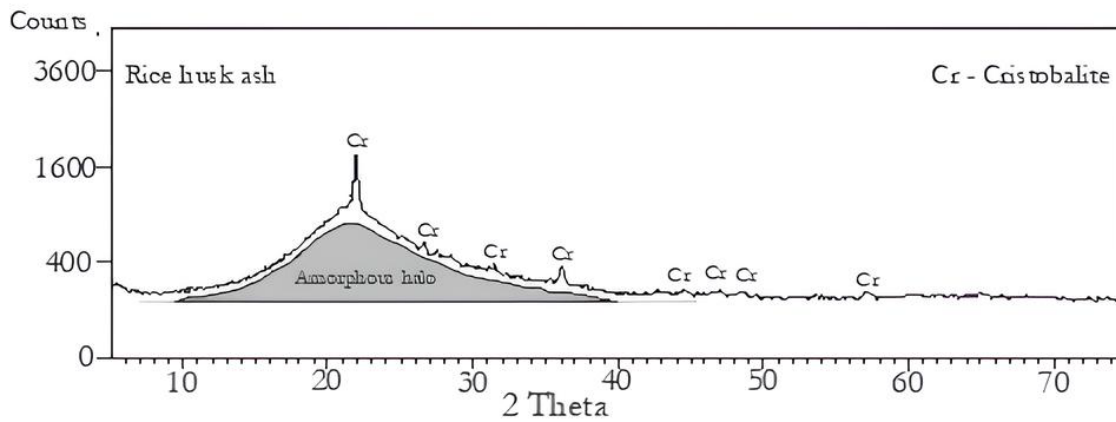


Figure 2. X-ray diffraction pattern of the mineral addition rice husk silica.

The fine and coarse aggregates used were natural sand and basalt origin crushed stone (crushed stone n.º “0”,  $d_{max} = 9.5$  mm), respectively. The granulometry data from NBR NM 248 (ABNT, 2003a) are shown in Figure 3, demonstrating compliance with NBR 7211 (ABNT, 2009) requirements.

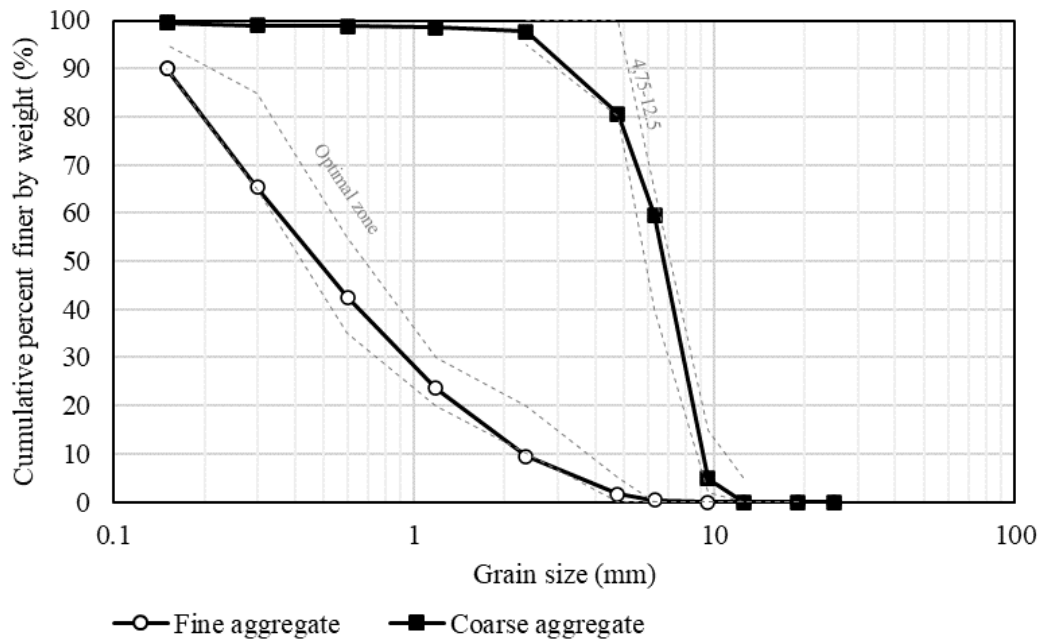


Figure 3. Granulometric curves of fine and coarse aggregates.

Table 3 shows the data for pulverulent material content according to NBR NM 46 (ABNT, 2003b); specific mass according to NBR NM 52 (ABNT, 2003c) for fine aggregate and NBR NM 53 (ABNT, 2006a) for coarse aggregate; unit mass according to NBR NM 45 (ABNT, 2006b); and absorption according to NBR NM 30 (ABNT, 2001). Although the pulverulent material content exceeded the limits for fine and coarse aggregates, 5% and 1%, respectively, it was understood that this characteristic would not interfere with the study's objectives.

Table 3. Characterization of aggregates used in concrete and mortars.

Property	Standard	Fine Aggregate	Coarse Aggregate
Fineness Modulus	NBR NM 248	2.33	5.79
Maximum Characteristic Dimension (mm)	NBR NM 248	4.75	9.5
Unit Mass (g/cm <sup>3</sup> )	NBR NM 45	1.60	2.39
Classification	NBR 7211	Optimal zone	4.15 – 12.5
Specific Mass (g/cm <sup>3</sup> )	NBR NM 52 and 53	2,510	2,747
Water Absorption	NBR NM 30	1.57%	1.59%
Pulverulent Material Content	NBR NM 46	5.33%	7.11%

Due to the low water/cement ratio used in the repair mortars, the superplasticizer additive PowerFlow 1180 from MC-Bauchemie, based on polycarboxylate polymers, with a density of 1.09 kg/L and a recommended dosage of 0.2% to 5.0% relative to cement mass, was added.

### 3.2 Production Process of Reinforced Concrete Specimens

For the experimental development of the study, corrosion potential and surface electrical resistivity tests were performed. These tests were applied to prismatic specimens simulating a repaired concrete piece, as illustrated in Figure 4.

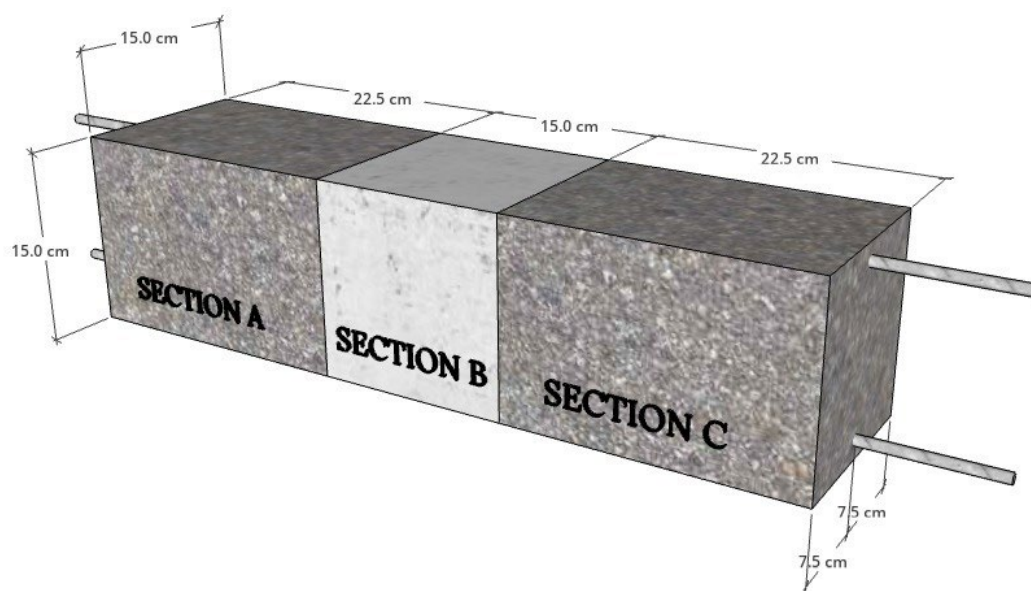


Figure 4. Prismatic reinforced concrete specimen repaired with mortar for incipient anode formation verification tests.

As illustrated in Figure 2, the reinforced concrete piece used for analysis was segmented into three sections: Section A, Section B, and Section C. This segmentation was performed to distinguish unrepaired regions from repaired regions during the tests. Sections A and C correspond to unrepaired regions, while Section B corresponds to the structural repair region.

The prismatic elements were molded with dimensions of 15 x 15 x 60 cm and were used by Daschevi (2022) in his master's thesis. The concrete was molded with Portland cement CPV – ARI and a mixing ratio, by mass, of 1:2.17:2.94:0.6 (cement: sand: crushed stone: water/cement ratio), with a cement consumption of 358 kg/m<sup>3</sup> and a mortar content of 51%, aiming for a characteristic



strength (fck) of 30 MPa at 28 days. Thus, this concrete had an average compressive strength of 37 MPa, an elastic modulus of 28 GPa, and an immersion absorption of 5.2%.

Additionally, a chloride contamination condition of 1.4% was considered, relative to cement mass, added as NaCl during concrete mixing in the mixer. This percentage corresponds to double the value used by Castro *et al.* (2003) to ensure reinforcement depassivation.

For the repair mortar, four mixing ratios were used:

- RHS (0%) Mixing Ratio: 1:3:0.4 (cement: sand: water/cement ratio).
- RHS (10%) Mixing Ratio: 0.90:0.10:3:0.4 (cement: RHS: sand: water/cement ratio).
- RHS (15%) Mixing Ratio: 0.85:0.15:3:0.4 (cement: RHS: sand: water/cement ratio).
- RHS (20%) Mixing Ratio: 0.80:0.20:3:0.4 (cement: RHS: sand: water/cement ratio).

The mortar consistency index was fixed at 200 mm  $\pm$  10 mm, obtained by adding 1.5% of superplasticizer additive based on polycarboxylate polymers relative to cement mass.

This experimental program also aimed to analyze a condition without repair. Table 4 shows the nomenclatures adopted for the examined specimens.

Table 4. Nomenclatures and specifications for the specimens.

Specimen	Repair	Addition	Substrate
RHS (0%) – Wt/Cl <sup>-</sup>	Yes	0%	Without Cl <sup>-</sup>
RHS (10%) – Wt/Cl <sup>-</sup>	Yes	10%	Without Cl <sup>-</sup>
RHS (15%) – Wt/Cl <sup>-</sup>	Yes	15%	Without Cl <sup>-</sup>
RHS (20%) – Wt/Cl <sup>-</sup>	Yes	20%	Without Cl <sup>-</sup>
RHS (0%) – W/Cl <sup>-</sup>	Yes	0%	1.4% Cl <sup>-</sup>
RHS (10%) – W/Cl <sup>-</sup>	Yes	10%	1.4% Cl <sup>-</sup>
RHS (15%) – W/Cl <sup>-</sup>	Yes	15%	1.4% Cl <sup>-</sup>
RHS (20%) – W/Cl <sup>-</sup>	Yes	20%	1.4% Cl <sup>-</sup>
Without repair – Wt/Cl <sup>-</sup>	Yes	-	Without Cl <sup>-</sup>
Without repair – W/Cl <sup>-</sup>	Yes	-	1.4% Cl <sup>-</sup>

The adopted steel bars were CA-50, with an 8 mm diameter, 70 cm length, and a nominal cover of 1 cm. Before molding, all bars were previously cleaned in a hydrochloric acid solution and hexamethylenetetramine, following the ASTM G-1 (1999) procedure. Then, all bars were rinsed in running water to remove the applied cleaning products and completely dried with paper towels. Additionally, the external regions of the bars were isolated, and conductor wires were soldered to them. On the other side of the wire, an electronic terminal was soldered to connect to the corrosion potential measurement device.

### 3.3 Corrosion Potential ( $E_{corr}$ )

According to Romano, Brito, and Rodrigues (2013), the corrosion potential of reinforcement in reinforced concrete is characterized by being a mixed potential, resulting from the kinetic combination of at least two processes: anodic oxidation of steel and reduction of dissolved oxygen. The corrosion potential test measures the potential difference between the reinforcement in the reinforced concrete structure and a reference electrode, which can maintain its fixed potential and serves as a comparison point (Medeiros *et al.*, 2013; Medeiros *et al.*, 2017).

The tests were conducted following ASTM C 876 (ASTM, 2015). Initially, this standard specifies that it does not address regions where concrete is located inside buildings and structures situated in the desert, as the structure can lose moisture and influence the concrete's resistivity, making it very high.

In this sense, the specimens were left in a water tank to avoid misleading results. Considering the need for moist concrete, the water present in the capillary porosity of reinforced concrete acts as a conductor, thus contributing to forming potential differences along the steel surface due to the presence of the aggressive agent (Song, Saraswarthy, 2007 *apud* Medeiros *et al.*, 2017). Therefore, the configuration adopted for the corrosion potential test included a voltmeter, a copper/copper sulfate reference electrode, conductors acting as negative and positive connections, and a wet sponge. Figure 5 shows the measurement system assembled for this experiment.



Figure 5. Equipment for conducting corrosion potential ( $E_{corr}$ ) tests.

Seven corrosion potential inspection points were conducted on the specimen's surface, four points on the unrepaired area, two points on the interface between the repair and concrete, and one point in the middle of the piece. The same procedure was adopted for the samples without repair. The configuration for conducting the tests can be observed in Figure 6.

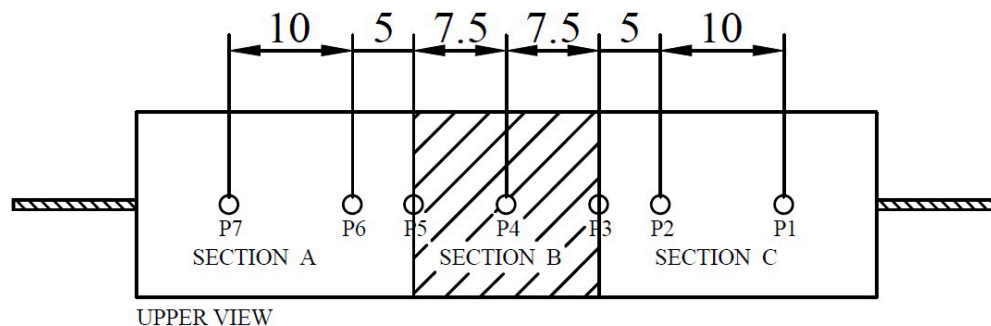


Figure 6. Corrosion potential analysis points.

Based on the obtained data, the probability of corrosion can be verified through Table 5 as presented in ASTM C 876 (ASTM, 2015).

Table 5. Probability of corrosion based on reinforcement corrosion potential (RCP) in the Specimen for readings using the Copper/copper sulfate electrode.

Value found	Probability of corrosion
PCA > - 200 mV	<10%
-350 mV < PCA < - 200 mV	Uncertain
PCA < - 350 mV	>90%

Source: ASTM C 876 (ASTM, 2015).

Furthermore, the corrosion potential test was conducted on both the upper and lower bars of each specimen.

### 3.4 Surface Electrical Resistivity

To obtain the surface electrical resistivity values of the concrete, the Four Electrode Method, also known as the Wenner Method, was used. This method is widely used in experiments involving concrete durability studies (Hornbostel, Larsen, Geiker, 2013; Medeiros Junior *et al.*, 2014; Medeiros Junior, Munhoz, Medeiros, 2019; Araújo *et al.*, 2022). This method was initially developed to determine soil's electrical resistivity (Silva, 2016).

For the surface electrical resistivity test, the Resipod equipment from Proceq was used. The test involves placing four electrodes on the concrete surface. The outer electrodes of the equipment emit an electric current, which can be alternating or direct, with a frequency of 40 Hz. According to the manufacturer, the current value can vary between 10 μA and 200 μA. The two internal electrodes measure the potential difference (ddp) resulting from the current applied by the external electrodes. The electrical resistivity is determined by (01) developed by Wenner.

$$\rho = 2\pi a \frac{V}{I} \tag{1}$$

Where:

ρ = Electrical resistivity of concrete (Ω.m);

a = Average distance between electrode axes (m);

V = Potential difference between internal electrodes (V);

I = Electric current (A).

Thus, two verifications of the concrete's surface electrical resistivity were conducted per sample section, both on the upper and lower surfaces. Figure 7 shows the analyzed points.

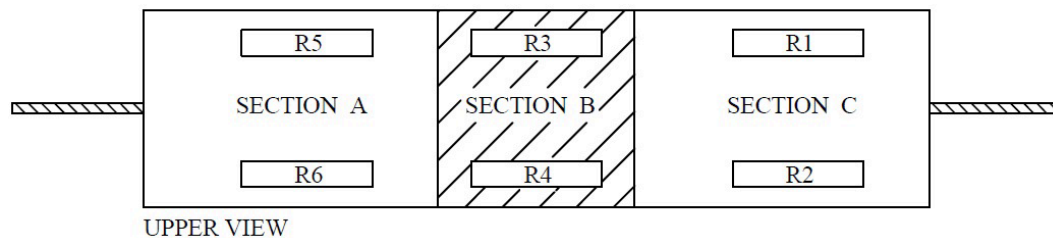


Figure 7. Surface electrical resistivity analysis points of concrete.

Based on the obtained results, Table 6 from the European Standard CEB 192 (CEB, 1989) was used to verify if the structure suffers any corrosion risk.

Table 6. Probability of corrosion risk.

Concrete Electrical Resistivity	Probability of Corrosion
$p > 20 \text{ kohm x cm}$	Negligible
$10 < p < 20 \text{ kohm x cm}$	Low
$5 < p < 10 \text{ kohm x cm}$	High
$p < 5 \text{ kohm x cm}$	Very High

Source: CEB 192 (CEB, 1989).

Although it is a simple and widely used technique, the Four Electrode Method must be applied carefully to avoid external influences, such as sample shape, electrode-concrete contact region, concrete heterogeneity, electrical wave type, frequency, and applied current intensity. These factors can impact measurement accuracy. Considering the used methodology, the next sections will present the results obtained through the tests.

## 4. RESULTS AND DISCUSSION

Corrosion in reinforced concrete elements can lead to a reduction in load-bearing capacity due to the decreased cross-sectional area of the steel and the development of cracks in the cementitious composites. Therefore, corrosion repairs and proper cleaning of the reinforcement are essential to prevent the recurrence of this pathological issue and the formation of incipient anodes. Given the limited discussion of this topic in the scientific literature (Castro et al., 2003; Christodoulou et al., 2013; Luković et al., 2017; Ali et al., 2018), none brought the use of rice husk silica in mortar repairs and if this could cause a formation of incipient anode in repaired areas. Therefore, the present study aimed to investigate the electrochemical differences caused by the use of rice husk silica in mortar repairs and whether this could potentially contribute to the formation of incipient anodes in reinforced concrete. The properties analyzed included physical characteristics (electrical resistivity, modulus of elasticity, and compressive strength) and physicochemical properties (corrosion potential). The results obtained for each test are presented in the following sections.

### 4.1 Substrate and Repair Mortar Characteristics

For comparison purposes with the characteristics of the repair mortars, the substrate concrete had an average strength of 37 MPa (standard deviation = 1.5 MPa) and an average elastic modulus of 28 GPa (standard deviation = 1.0 GPa).

Figure 8 shows the compressive strength variation of the mortars with the RHS content variation. It should be noted that the mortar with 10% partial replacement of cement with RHS showed an 11.6% increase in compressive strength compared to the reference mortar. In the case of 15% and 20% replacement percentages, there was a reduction in strength of 10.0% and 43.6%, respectively, compared to the reference mortar.

Overall, there was a tendency to reduce strength with the increased partial replacement of cement with RHS. Comparing the strength data with the substrate concrete that received the repair (37 MPa), it is essential to note that only the 20% RHS mortar had a lower compressive strength than the substrate.

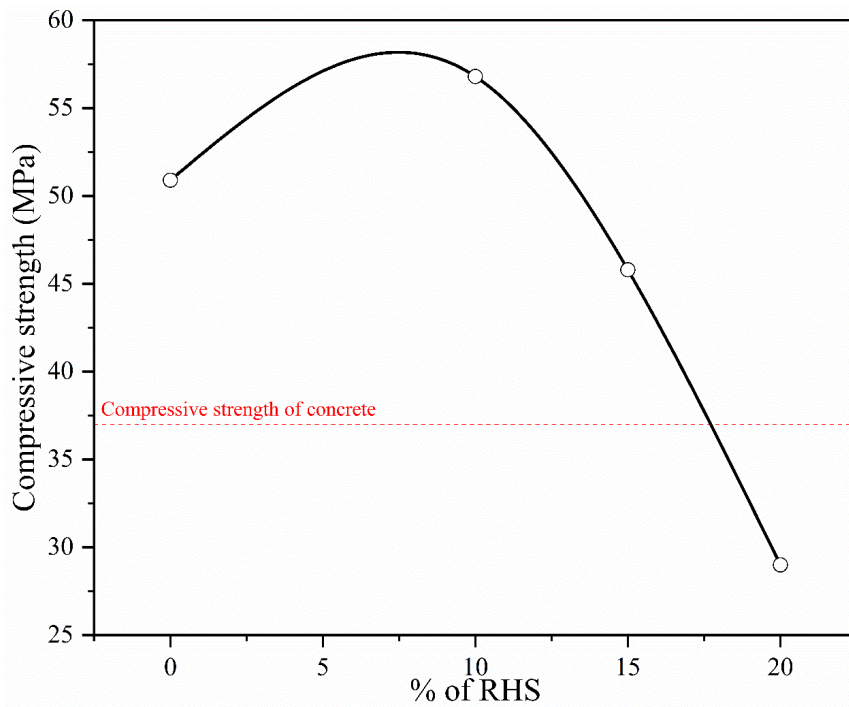


Figure 8. Compressive strength of mortars as a function of RHS content, measured on 40 x 40 x 80 cm specimens, at 28 days of curing.

Figure 9 shows the influence of partial cement replacement with RHS on the average elastic modulus values at 28 days. The statistical analysis indicated that the averages of 0%, 10%, and 15% have no significant difference, being considered similar. On the other hand, the 20% content caused a statistically significant reduction, representing a 5.6% decrease compared to the 0% content. It should be noted that all mortars have a higher elastic modulus than the substrate, which is 28 GPa.

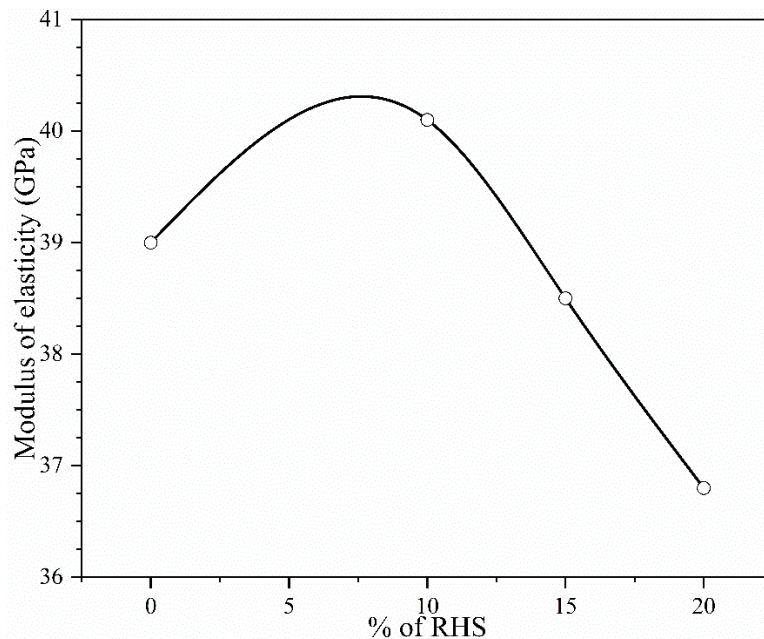


Figure 9. Static elastic modulus of mortars as a function of RHS content, measured on 40 x 40 x 160 cm specimens, at 28 days of curing.

## 4.2 Corrosion Potential

The corrosion potential test is used to evaluate a material's propensity to corrosion in a specific environment or condition. The data obtained from this test were transformed into arithmetic means, as there was not much variation in corrosion potential at the 7 inspection points along the concrete piece. The analysis revealed a standard deviation between 3 and 10 and a coefficient of variation of 1% to 9%. Figure 10 shows the  $E_{corr}$  values as a function of the specimens of each test series.

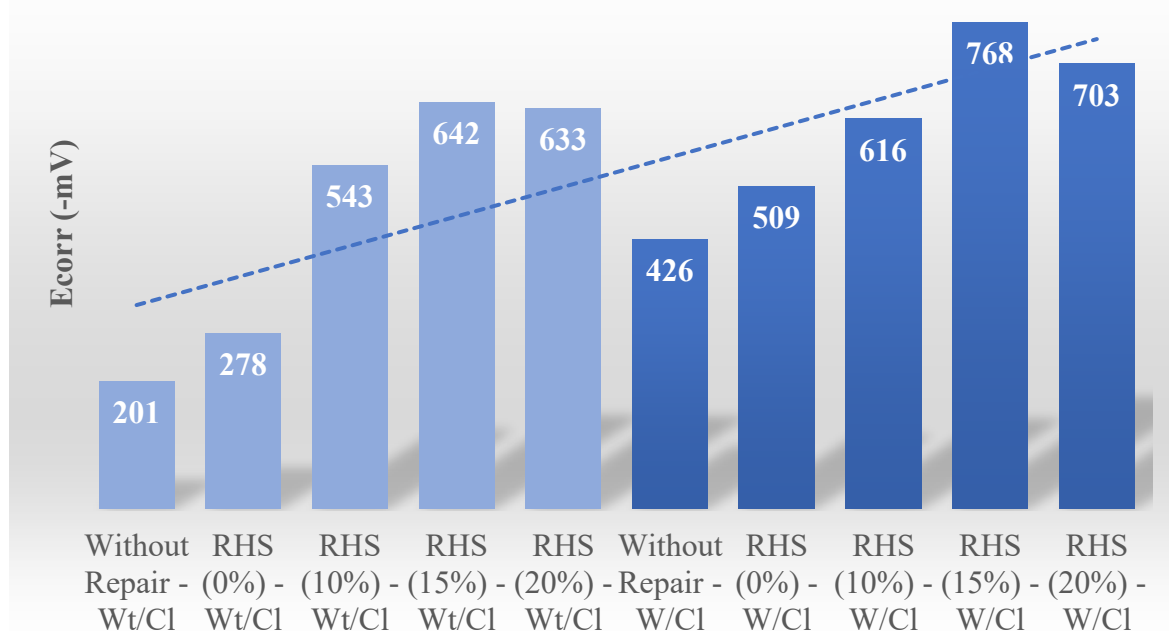


Figure 10. Corrosion potential using a copper/copper sulfate reference electrode.

To analyze Figure 10, it is helpful to interpret it in parts. Initially, the specimens without repair, with and without chloride contamination, should be observed. In this case, the influence of the contaminant presence is evident, making the results more electronegative in the presence of chloride ions. According to ASTM C 876 (ASTM, 2015) classification, it can be stated that the non-contaminated case has less than 10% probability of corrosion. In the case of concrete contaminated with chlorides, it can be stated that there is more than a 90% probability of corrosion, meaning that the 1.4% chloride contamination relative to cement mass caused more than a 100% alteration of the  $E_{corr}$  values.

Focusing on Figure 10 with an emphasis on the chloride-contaminated series, it is observed that localized repair did not improve corrosion potential values, keeping the repaired pieces at  $E_{corr}$  values indicating more than a 90% probability of corrosion. This means that the localized repair did not ensure the installed corrosion process's stagnation, continuing to develop and advance in the repaired concrete. Furthermore, analyzing Figure 10 and comparing the case of modified repair mortar with a high-reactivity pozzolan, the  $E_{corr}$  values were even more electronegative, varying between 21% and 51% compared to the mortar repair without RHS. This is an alert since using a pozzolan, which is usually expected to improve the repair, may result in worse performance under service conditions.

Analyzing Figure 10 focusing on the non-chloride-contaminated series, it should be noted that the repair introduction causes some electrochemical disturbance, making the repaired concrete pieces show more electronegative  $E_{corr}$  values compared to the series without repair and without chlorides. The RHS (15%) – S/Cl series should be highlighted, whose  $E_{corr}$  value was -642 mV,

219% more electronegative than the piece without repair and without chlorides.

An explanation for the increased  $E_{corr}$  electronegativity with RHS in mortars is that this high-reactivity pozzolan considerably consumes the portlandite resulting from the cement hydration process, as demonstrated in the works of Hoppe Filho *et al.* (2017) and Campos, Medeiros, and Hoppe Filho (2022). However, it is interesting to emphasize that the calcium silicate hydrate formed through the pozzolanic reaction has a lower density than the C-S-H formed during the Portland cement hydration process (Ribeiro, 2018). In this sense, there is a probability that using RHS, the portlandite responsible for the mortar's high pH was consumed, generating a pH reduction in the repair mortar and causing electrochemical incompatibility with the substrate concrete.

The environment's pH significantly impacts the equilibrium potentials, with a high pH resulting in more electronegative equilibrium potentials. An increase of just one unit in the alkaline region's pH in concrete results in a more negative 60 mV change in equilibrium potentials between steel and products, as well as equilibrium potentials for oxygen and hydrogen reactions (Pourbaix, 1990 *apud* Christodoulou *et al.*, 2013).

### 4.3 Surface Electrical Resistivity

Figure 11 and 12 shows the obtained data for the surface electrical resistivity of the materials that make up the repaired reinforced concrete specimens. It should be noted that the surface electrical resistivities of the repair mortars are higher compared to the substrate concrete, and this difference can be a trigger for incipient anode formation.

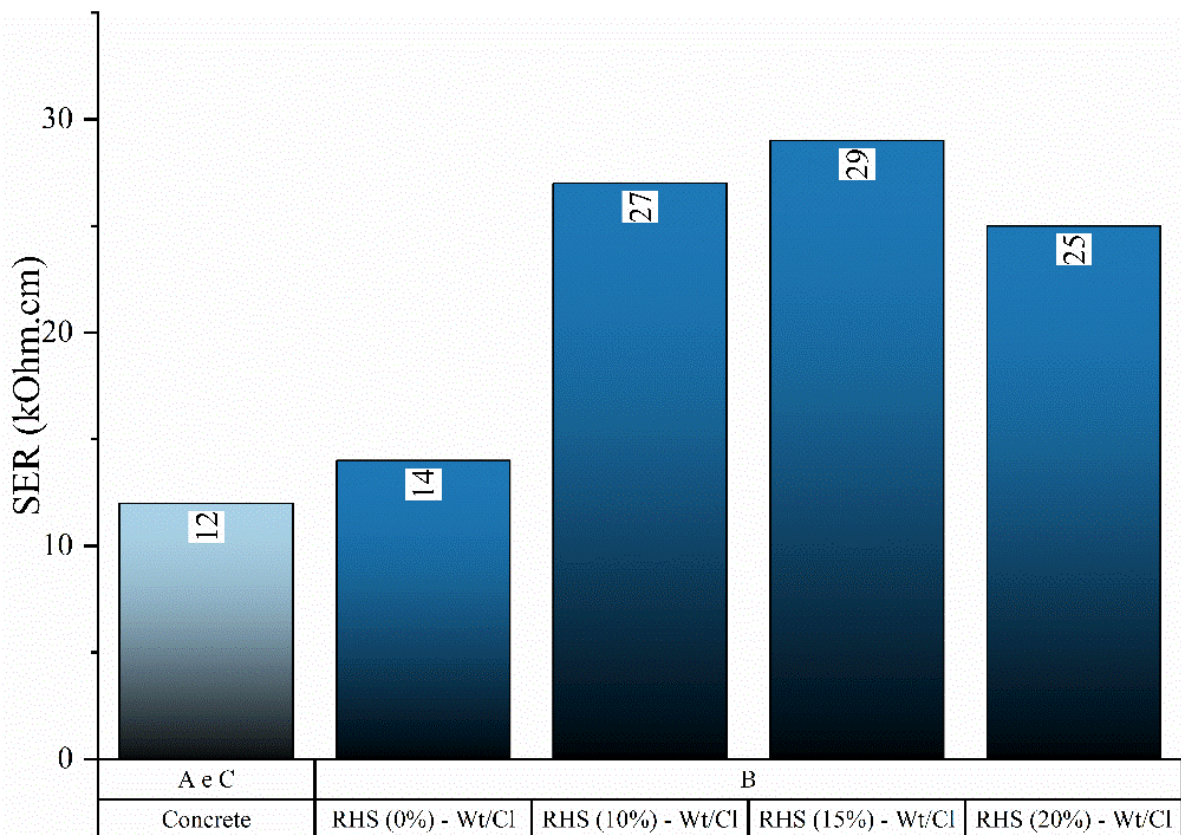


Figure 11. Surface electrical resistivity (SER) of the specimens without chloride.

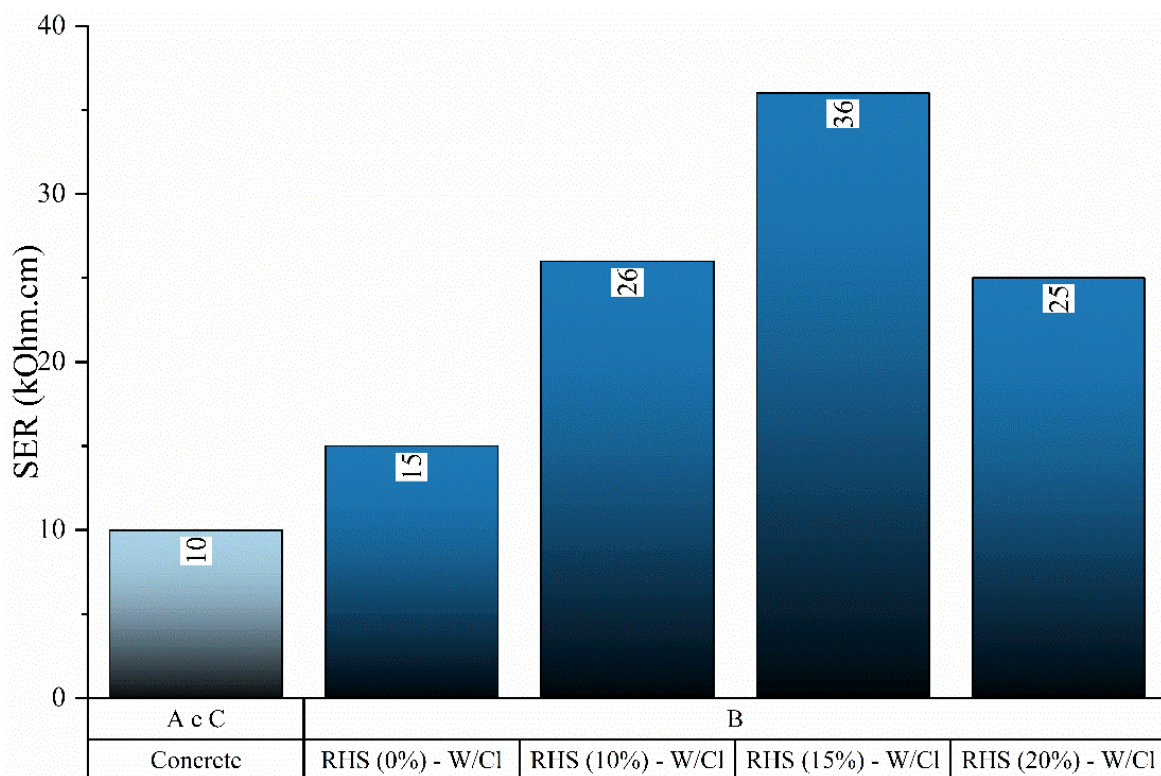


Figure 12. Surface electrical resistivity (SER) of the specimens with chloride.

The surface electrical resistivity (SER) results align with those obtained in the studies by Wosniack *et al.* (2021) and Araújo, Macioski, and Medeiros (2022), which also observed higher electrical resistivity values for concretes molded with rice husk silica compared to concretes without this addition. Concrete's electrical resistivity is related to the cement matrix's microstructure, including pore structures, porosity, and its distribution. These properties are controlled by the cement's degree of hydration (Polder, 2001, *apud* Silva, Ferreira, Figueiras, 2011). For this reason, high surface electrical resistivity values for repair mortars with rice husk silica are observed compared to the substrate concrete and mortar without RHS.

In this sense, as Wosniack *et al.* (2021) state, pozzolanic activity impacts concrete's surface electrical resistivity, refining the pores and contributing to a denser paste. Another effect of pozzolanic addition reported in the works of Medeiros *et al.* (2013) and Medeiros Junior, Munhoz and Medeiros (2019) impacting cementitious composites' electrical resistivity is calcium hydroxide consumption in the pozzolanic reaction, making the concrete pore solution less concentrated in  $\text{Ca}^{2+}$  and  $\text{OH}^-$  ions and consequently less conductive or more resistive. These arguments explain why the electrical resistivity values in mortars with RHS are much higher than materials without RHS (reference mortar and substrate concrete).

However, it is important to emphasize that, as determined by Hoppe Filho *et al.* (2017), who analyzed the pozzolanic activity index with lime according to NBR 5751 (ABNT, 2015), rice husk silica has lower pozzolanic activity kinetics compared to active silica and metakaolin. Therefore, using other additions would result in different surface electrical resistivity values for the repair mortar.

Returning to this work, which deals with repaired concrete specimens, in the case of repair mortar without rice husk silica addition, the surface electrical resistivity values were 17% higher in the repaired region than in the substrate concrete region. This is due to the repair mortar having a lower water/cement ratio than the substrate concrete (neighboring regions). According to the results obtained by Chen and Wu (2013), porosity increases as the water/cement ratio increases, and according to Medeiros Junior, Munhoz and Medeiros (2019), resistivity decreases as the



water/cement ratio increases. Therefore, the data obtained in the experimental campaign are consistent, as the surface electrical resistivity of repair mortar without RHS is higher due to a denser mixture.

However, the previously explained effects show that adding RHS causes a greater RES difference between the repaired substrate and the repair filling mortar. On this subject, Figure 13 shows that mortars with RHS, consequently with a greater RES difference between the substrate and the mortar, result in more electronegative values of the repaired system, indicating a greater tendency for corrosion due to the electrochemical incompatibility between the regions.

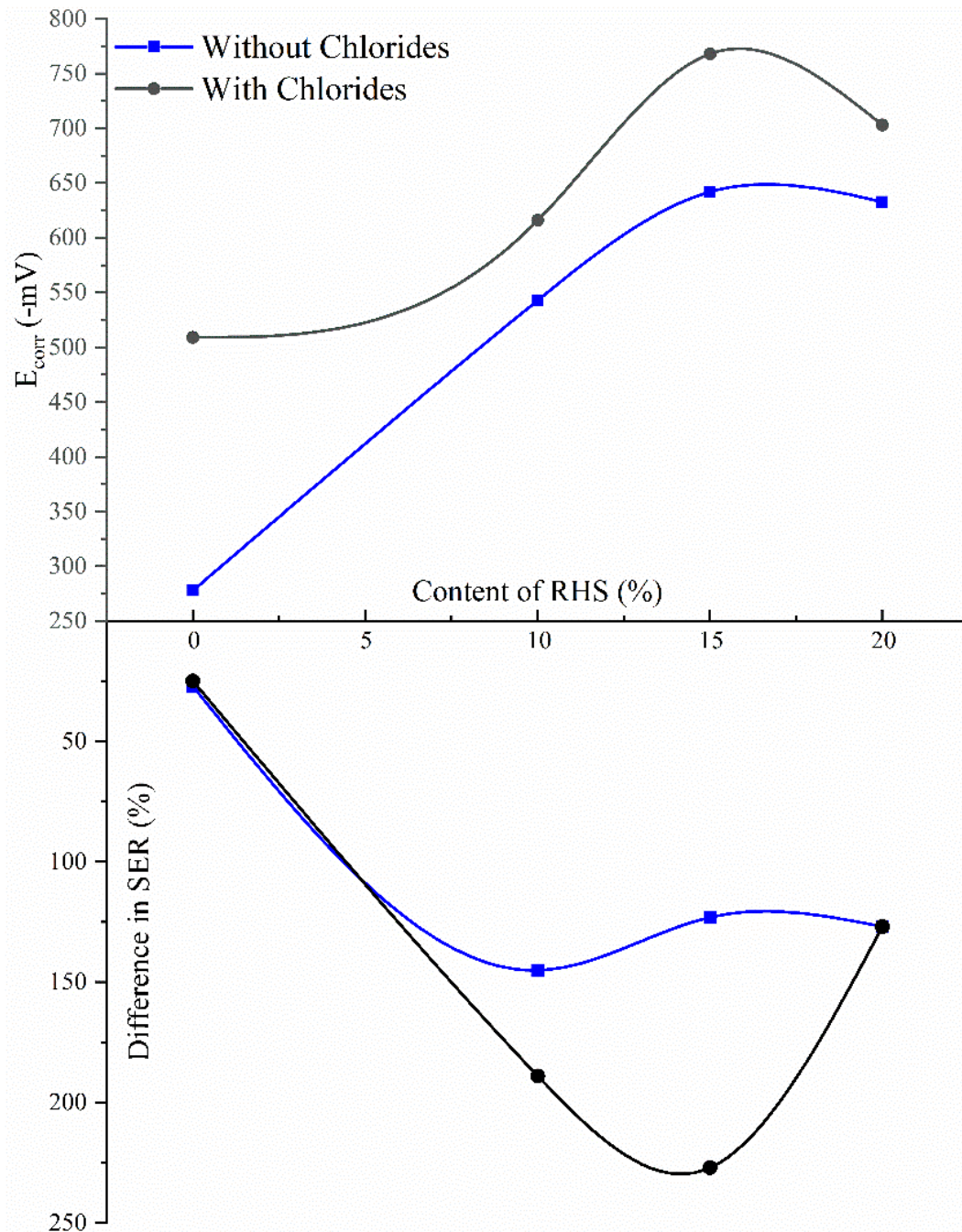


Figure 13. Relationship between RHS content,  $E_{corr}$ , and the RES difference between the substrate concrete and repair mortar.

## 5. CONCLUSIONS

From the experimental plan developed in this work, the following considerations can be made:

- Adding rice husk silica (RHS) caused an increase in the repair mortars' electrical resistivity, with increases ranging from 67% to 140% compared to the mortar without RHS.
- It is verified that only with corrosion potential data it would not be possible to affirm the existence of the incipient anode phenomenon, as the steel's corrosion potential showed little variation inside and outside the repair.
- Evaluating the surface electrical resistivity data, it is possible to note the difference in properties between the repair mortar and concrete, especially in the case of mortar with RHS addition.
- It is essential to emphasize that when analyzing the possibility of incipient anode existence in structural elements, only one testing method should not be used, as having data from different experiments provides more certainty about the phenomenon's occurrence. In view of this, to ensure the occurrence of corrosion in the samples, it would be necessary to include measurements of corrosion rate and galvanic current.
- The localized repair introduced in the specimens caused corrosion potential movements to more electronegative values, indicating a probability of active corrosion happening, even in cases where the substrate was not contaminated by chlorides.
- The main conclusion of this work is that adding rice husk silica to the repair mortar resulted in greater surface electrical resistivity differences between the repaired area and the concrete substrate sections, making the corrosion potential values of repaired pieces more electronegative, indicating a tendency for reinforcement corrosion failure caused by incipient anode formation.

## 6. ACKNOWLEDGEMENTS

The authors express their gratitude to the Brazilian agencies CNPq, Capes, and Fundação Araucária for the scholarship and financial support, the Federal University of Paraná (UFPR) campus Curitiba, Polytechnic Center, Civil Construction Department (DCC), Graduate Program in Civil Engineering (PPGEC), Civil Engineering Studies Center (CESEC), Materials and Structures Laboratory (LAME), Pathology and Construction Recovery Research Group (PRC), as well as the Pilecco Nobre Group and Cia. de Cimentos Itambé for donating materials for the research.

## 7. REFERENCES

- Associação Brasileira de Normas Técnicas (2015), NBR 5751 – Materiais pozolânicos – Determinação da atividade pozolânica com cal aos sete dias. Rio de Janeiro.
- Associação Brasileira de Normas Técnicas (2018), *NBR 16697 - Cimento Portland - Requisitos*. Rio de Janeiro.
- Associação Brasileira de Normas Técnicas (2010), *NBR 15895: Materiais pozolânicos – Determinação do teor de hidróxido de cálcio fixado – Método Chapelle modificado*. Rio de Janeiro.
- Associação Brasileira de Normas Técnicas (2009), *NBR 7211 - Agregados para concreto - Especificação*. Rio de Janeiro.
- Associação Brasileira de Normas Técnicas (2001), *NBR NM 30 - Agregado miúdo - Determinação da absorção de água*. Rio de Janeiro.
- Associação Brasileira de Normas Técnicas (2006b), *NBR NM 45 - Agregados - Determinação da massa unitária e do volume de vazios*. Rio de Janeiro.

- Associação Brasileira de Normas Técnicas (2003b), *NBR NM 46 - Agregados - Determinação do material fino que passa através da peneira 75 um, por lavagem*. Rio de Janeiro.
- Associação Brasileira de Normas Técnicas (2003c), *NBR NM 52 - Agregados miúdo - Determinação da massa específica e massa específica aparente*. Rio de Janeiro.
- Associação Brasileira de Normas Técnicas (2006a), *NBR NM 53 – Agregado graúdo – Determinação de massa específica, massa específica aparente e absorção de água*. Rio de Janeiro.
- Associação Brasileira de Normas Técnicas (2003a), *NBR NM 248 - Análise Granulométrica*. Rio de Janeiro.
- American Society for Testing and Materials (1999), *ASTM G1 - Standard Practice for Preparing, Cleaning, and Evaluation Corrosion Test Specimens*. Philadelphia.
- American Society for Testing and Materials (2015), *ASTM C-876: Standard Test Method for Corrosion Potentials of Uncoated Reinforcing Steel in Concrete*. Philadelphia.
- Ali, M. S. et al. (2018), *An experimental study of electrochemical incompatibility between repaired patch concrete and existing old concrete*. *Construction and Building Materials*, v. 174, p. 159-172. <https://doi.org/10.1016/j.conbuildmat.2018.04.059>
- Araújo, E. C., Macioski, G., De Medeiros, M. H. F. (2022), *Concrete surface electrical resistivity: Effects of sample size, geometry, probe spacing and SCMs*. *Construction and Building Materials*, v. 324, p. 126659. <https://doi.org/10.1016/j.conbuildmat.2022.126659>
- Campos, P. A., Medeiros, M. H. F., Filho, J. H. (2022), *Ação conjugada de sílica de casca de arroz e hidróxido de cálcio em compósitos de cimento Portland: porosidade, compostos hidratados, reserva alcalina, e resistência à compressão*. *Revista Matéria*, v. 27, n.03. <https://doi.org/10.1590/1517-7076-RMAT-2022-0018>
- Castro, P., Pazini, E., Andrade, C., Alonso, C. (2003), *Macrocell activity in slightly chloride-contaminated concrete induced by reinforcement primers*. *Corrosion*, v. 59, n. 6, p. 535–546. <https://doi.org/10.5006/1.3277585>
- Comité Euro-Internacional du Béton (1989), *Nº 192: diagnosis and assessment of concrete structures: state-of-art report*. Switzerland: FIB – International Federation for Structural Concrete.
- Chen, X., Wu, S. (2013), *Influence of water-to-cement ratio and curing period on pore structure of cement mortar*. *Construction and Building Materials*, v.38, p. 804-812. <https://doi.org/10.1016/j.conbuildmat.2012.09.058>
- Christodoulou, C., et al. (2013), *Diagnosing the cause of incipient anodes in repaired reinforced concrete structures*. *Corrosion Science*, v. 69, p. 123 – 129. <https://doi.org/10.1016/j.corsci.2012.11.032>
- Daschevi, P. A. (2022), *‘Efeito do ânodo incipiente em reparos localizados utilizando argamassas com substituição parcial de ligante por sílica de casca de arroz’*. Tese de mestrado, Universidade Federal do Paraná, Curitiba.
- Hoppe Filho, J. et al. (2017), *Atividade pozolânica de adições minerais para cimento Portland (Parte I): Índice de atividade pozolânica (IAP) com cal, difração de raios-X (DRX), termogravimetria (TG/DTG) e Chapelle modificado*. *Revista Matéria*, v. 22, n. 03. <https://doi.org/10.1590/S1517-707620170003.0206>
- Hoppe Filho, J. et al. (2017), *Reactivity Assessment of Residual Rice-Husk Ashes*. *Journal of Materials in Civil Engineering*, v. 1, p. 04017003. [https://doi.org/10.1061/\(ASCE\)MT.1943-5533.000182](https://doi.org/10.1061/(ASCE)MT.1943-5533.000182)
- Grandes Construções (2017), *Brasil perde 4% do PIB com corrosão*. *Revista Grandes Construções*.
- Hornbostel, K., Larsen, C. K.; Geiker, M. R. (2013), *Relationship between concrete resistivity and corrosion rate—A literature review*. *Cement and concrete composites*, v. 39, p. 60-72. <https://doi.org/10.1016/j.cemconcomp.2013.03.019>
- Kamde, D. K., et al. (2021), *Long-term performance of galvanic anodes for the protection of steel reinforced concrete structures*. *Journal of Building Engineering*, v. 42, p. 103049. <https://doi.org/10.1016/j.jobe.2021.103049>

- Luković, M., et al. (2017), *Failure Modes in Concrete Repair Systems due to Ongoing Corrosion*. Hindawi, Advances in Materials Science and Engineering. <https://doi.org/10.1155/2017/9649187>
- Mehta, P. K., Monteiro, P. J. M. (2008), “*Concreto: Microestrutura, Propriedades e Materiais*”. Ibracon.
- Medeiros, M. H. F., et al. (2013), *Inspection of Buildings in Rio de Janeiro-Brazil: Proving the greater tendency of corrosion at the base of reinforced concrete columns using potential corrosion technique*. American Journal of Engineering Research (AJER), v. 2, p. 102-112.
- Medeiros, M. H. F., et al. (2017), *Potencial de corrosão: influência da umidade, relação água/cimento, teor de cloretos e cobrimento*. Revista Ibracon de Estruturas e Materiais, v.10, p. 864-885. <https://doi.org/10.1590/S1983-41952017000400005>
- Medeiros, M. H. F., et al. (2013), *High-Volume Fly Ash Concrete with and without Hydrated Lime: Chloride Diffusion Coefficient from Accelerated Test*. Journal of Materials in Civil Engineering, v. 25, p. 411 - 418. [https://doi.org/10.1061/\(ASCE\)MT.1943-5533.000059](https://doi.org/10.1061/(ASCE)MT.1943-5533.000059)
- Medeiros, M. H. F., et al. (2017), *Corrosion potential: influence of moisture, water-cement ratio, chloride content and concrete cover*. REVISTA IBRACON DE ESTRUTURAS E MATERIAIS, v. 10, p. 864-885. <https://doi.org/10.1590/S1983-41952017000400005>
- Medeiros, M. H. F., Daschevi, P. A., Araújo, E. C. (2022), *Reparo localizado para estruturas de concreto armado: erros, acertos e reflexões*. Concreto & Construções. <https://doi.org/10.4322/1809-7197.2022.106.0001>
- Medeiros Junior, R. A., et al. (2014), *Investigação da resistência à compressão e da resistividade elétrica de concretos com diferentes tipos de cimento*. Revista ALCONPAT, v. 4, p. 116-128. <https://doi.org/10.21041/ra.v4i2.21>
- Medeiros Junior, R. A., Munhoz, G. S., Medeiros, M. H. F. (2019), *Correlations between water absorption, electrical resistivity and compressive strength of concrete with different contents of pozzolan*. Revista ALCONPAT, v. 9, p. 152-166. <https://doi.org/10.21041/ra.v9i2.335>
- Nace International (2016), *International Measures of Prevention Application, and Economics of Corrosion Technologies Study*.
- Romano, P., Brito, P. S. D., Rodrigues, L. (2013), *Monitoring of the degradation of concrete structures in environments containing chloride ions*. Construction and Building Material, v. 47, p. 827 – 832. <https://doi.org/10.1016/j.conbuildmat.2013.05.042>
- Silva, P. C., Ferreira, R. M., Figueiras, H. (2011), “*Electrical Resistivity as a Means of Quality Control of Concrete – Influence of Test Procedure*”. International Conference on Durability of Building Materials and Components.
- Silva, L. M. A. (2016), “*Resistividade elétrica superficial do concreto: influência da cura*”. Trabalho de conclusão de curso, Universidade Federal de Goiás.
- Ribeiro, D. V. (2018), *Estruturas dos poros e mecanismos de transporte no concreto*. In: Ribeiro, D. V., et al. “*Corrosão e Degradação em Estruturas de Concreto*”. Rio de Janeiro: GEN, p. 51-93.
- Wosniack, L. M. et al. (2021), *Resistividade elétrica do concreto pelo ensaio de migração de cloretos: comparação com o método dos quatro eletrodos*. Ambiente Construído, Porto Alegre, v. 21, n. 3, p. 321 – 340. <https://doi.org/10.1590/s1678-86212021000300554>